Breast Cancer: Targets and Therapy

Dovepress
open access to scientific and medical research

Open Access Full Text Article

ORIGINAL RESEARCH

Potentiating the Cytotoxic Activity of a Novel Simvastatin-Loaded Cubosome against Breast Cancer Cells: Insights on Dual Cell Death via Ferroptosis and Apoptosis

Yara E Elakkad[1]
Shimaa Nabil Senousy Mohamed[2]
Nermeen Z Abuelezz[3]

[1]Department of Pharmaceutics, College of Pharmaceutical Sciences and Drug Manufacturing, Misr University for Science and Technology, Giza, Egypt; [2]Biochemistry Division, Chemistry Department, Center of Basic Sciences, Misr University for Science and Technology, Giza, Egypt; [3]Biochemistry Department, College of Pharmaceutical Sciences and Drug Manufacturing, Misr University for Science and Technology, Giza, Egypt

Purpose: Female breast cancer is the most prevalent cancer worldwide. Emerging evidence shows that simvastatin (SIM) has promising anticancer activities. However, the underlying mechanisms are not fully elucidated. Increasing reports imply statins can modulate ferroptosis through disrupting reactive oxygen species (ROS) and glutathione peroxidase enzyme (GPX4) levels. However, whether ferroptosis contributes to SIM anticancer activity, especially regarding GPX4 is unclear. Moreover, poor aqueous SIM solubility hinders its delivery in adequate levels to tumor sites. Meanwhile, cubosomes are biocompatible nanocarriers that enhance lipophilic drug delivery. Therefore, in this study, we formulated a novel SIM-loaded cubosome (SIM-CB) and analyzed its cytotoxic activity on MCF-7 cancer cells in comparison with free SIM.

Methods: The present study tested the cytotoxic activity of SIM-CB on MCF-7 cells, in comparison with SIM using sulphorhodamine assay. We analyzed SIM-CB effect on apoptosis and cell cycle using flowcytometry, and investigated its effect on Bcl-2, caspase 3, ROS, reduced glutathione (GSH), lipid peroxides and GPX4 enzyme. Finally, we tested the persistence of SIM-CB apoptosis and ferroptosis activities on MCF-7 cells in presence of vitamin E, a potent antioxidant and ferroptosis inhibitor.

Results: SIM-CB was successfully formulated at the nano size. SIM-CB significantly increased simvastatin therapeutic activity, with IC_{50} of SIM-CB 52% lower than SIM. 95% CI [1.8, 2.7], SD = 0.34 for SIM-CB, and [4.1, 5.2], SD = 0.45 for SIM. Compared with free SIM, SIM-CB doubled total deaths and increased apoptosis ($p < 0.05$). Moreover, SIM-CB remarkably increased caspase-3, ROS, and lipid peroxide levels but decreased antiapoptotic Bcl-2 protein, GSH, and GPX4 compared with free SIM. Notably, SIM-CB elicited a high distinguished resistance against the inhibitory effects of vitamin E.

Conclusion: To the best of our knowledge, this study is the first to present SIM-CB as a promising means to enhancing the therapeutic potential of simvastatin against breast cancer cells, through potentiating both apoptosis and ferroptosis.

Keywords: anticancer, MCF-7 breast cancer cells, statins, nanoparticle, cell death

Correspondence: Nermeen Z Abuelezz
Biochemistry Department, College of Pharmaceutical Sciences and Drug Manufacturing, Misr University for Science and Technology, Giza, Egypt
Tel +20 1005677429
Email nermeenzak01@gmail.com

Introduction

Female breast cancer is the most prevalent cancer type and one of the top three deadliest cancers worldwide.[1] Despite the remarkable progress in breast cancer treatment, considerable number of cases still suffer from prompt recurrence, poor prognosis and metastasis.[2] Therefore, extensive efforts are ongoing to integrate novel agents that can

Received: 6 September 2021
Accepted: 29 November 2021
Published: 14 December 2021

tackle these challenges. Statins are drugs widely used to control hypercholesterolemia, through inhibiting the rate limiting (HMG-COA reductase step) of cholesterol synthesis. Recent studies spot the distinguished potential of lipophilic statins, against different cancer types.[3,4] In agreement, simvastatin (SIM) use is reported to decrease the risk of breast cancer progression to higher stages.[5,6] While other basic studies reveal that SIM potentiates the cytotoxic effects of anticancer drugs against MCF-7 cells.[7] The cytotoxic potential of SIM has been explained mostly by its ability to induce apoptosis and modulate protein cascades that regulate the apoptotic pathway in tumor cells.[8–10] However, to date, the mechanisms underlying SIM cytotoxic activity are not fully clarified. Ferroptosis is currently emerging as a significant type of programmed cell death that encounters cancer progression and possible anticancer activity.[11] Where, on the molecular level, the proper levels and functionality of reduced glutathione (GSH) and subcellular phospholipid hydroperoxide glutathione peroxidase (GPX4) enzyme are the core of keeping ferroptosis in check. Whereas ferroptosis inducers act to reduce or destabilize GPX4 enzyme and deplete GSH stores.[12] Such changes consequently enhance the membranous lipid peroxidation and cause the accumulation of reactive oxygen species (ROS), which elevate ferrous ion oxidation (Fe^{2+}), eventually increasing ferroptosis.[13] Increasing evidence strongly suggests the ferroptotic potential of lipophilic statins through inhibiting mevalonate pathway and increasing cellular lipid peroxidation.[14,15] Remarkably, the upregulation of mevalonate pathway is repeatedly reported in breast cancer.[16,17] Therefore, given these observations, modulating ferroptosis can constitute an additional potent mechanism for the anticancer activity of simvastatin. However, to date, limited data are available about the effect of SIM on GPX4 level in breast cancer, and whether this probable ferroptosis activity contributes to the anticancer potential of SIM against breast cancer. Additionally, to exert an anticancer activity, a high dose of statins is often needed. However, the poor aqueous solubility and rapid elimination of oral free SIM often hinders its proper delivery to the tumor sites in adequate concentrations and also decreases its bioavailability.[18,19]

In this regard, the incorporation of poor water-soluble drugs in nano vesicular structures presents an innovative way to enhance the delivery and efficacy of lipophilic anticancer drugs, while reducing their side effects, controlling their release and increasing their bioavailability.[20,21] Non-lamellar liquid crystalline lipid phase (LCP) nanoparticles like cubosomes, have multiple advantages over planner structures and liposomes in this aspect. Cubosomes provide larger membrane surface area to nanoparticle volume and therefore permit high loading capacity of drugs due to their enormous lipid-water interface which increases the delivered dose and bioavailability of lipophilic drugs.[22] Cubosomes are also less viscous suspensions, which makes ease their handling and delivery to the appropriate tumor sites. Among lipid nanoparticles, cubosomes have a distinguished ability to release the loaded drugs in a controlled and a sustained release pattern. Compared with liposomes, cubosomes exert a higher stability and a larger ratio of bilayer area to particle volume, which facilitates the interaction with the lipid bilayer structure of cells.[23] Interestingly, cubosomes maintain a stable three-dimensional structure under a range of physiologically relevant conditions which provide a highly efficient penetration power in cancerous cells.[24] Therefore, in the present study, we formulated a novel biocompatible SIM-loaded cubosome nanoparticle (SIM-CB), in attempt to enhance the anticancer potential of SIM, and maximize the advantage of SIM lipophilicity as a promising ferroptosis inducer. Secondly, we analyzed the apoptosis and ferroptosis activity of both free simvastatin (SIM) and the formulated SIM-CB on MCF-7 breast cancer adenoma cells. Finally, we investigated the persistence of apoptotic and ferroptotic activities of SIM and SIM-CB in the presence of vitamin E which is a potent antioxidant and a ferroptosis inhibitor.[25–27] Clarifying the cytotoxic properties of SIM-loaded cubosome may consequently provide a good opportunity to further optimize the off-label activity of SIM-CB as a promising systemic (intravenous) anticancer agent against persistent breast cancer.

Materials and Methods

Chemicals

Simvastatin was a kind gift from Amriya Pharmaceutical Company (Egypt). Glyceryl mono oleate (GMO) and Pluronic F127 were obtained from Sigma Aldrich Chemie GmbH, (Switzerland). Deionized water was obtained from Arab Company for Pharmaceutical and Medicinal plants (MEPACO-MEDIFOOD, Egypt). Absolute ethyl alcohol, methyl alcohol, potassium dihydrogen phosphate and disodium hydrogen phosphate were obtained from El Nasr Pharmaceutical Chemicals (Egypt). All used chemicals were of analytical grade.

Cell Line

Human breast carcinoma cell line MCF-7 was obtained from American Type Culture Collection (ATCC, Chicago,

IL, USA) and cultured using Dulbecco's modified Eagle's medium (DMEM) with glutamine (Lonza, EU), supplemented with 10% heat-inactivated fetal bovine serum (FBS) (Lonza, EU) and 1% Penicillin-Streptomycin (Lonza, EU). Cells were maintained in humidified, 5% CO_2 at 37°C and passaged upon reaching 70–80% confluency, using a mixture of 0.25% Trypsin- 0.53 mM EDTA (Lonza, E.U.). Cultured cells at third to fifth passages were used for analysis.

Formulation of Simvastatin Cubosome Nano Dispersion (SIM-CB)

Cubosomes were prepared with reference to the established method,[28,29] using glyceryl monooleate (GMO) as the structure-forming lipid and Pluronic F127 as the emulsifier and surfactant stabilizing the cubosome dispersion. For breast cancer cells, a formula of size less than 200 nm, high drug entrapment efficiency, high zeta potential and homogenous mono dispersion of polydispersity index (PDI) less than 0.3 would constitute preferable criteria.[30,31] Accordingly, different ratios of GMO to Pluronic F 127 (W:W) were tried to reach the targeted criteria. GMO and Pluronic F127 were mixed and molten using magnetic stirrer hot plate at 60°C. For drug encapsulation, simvastatin was added to the molten mixture of lipid and surfactant to give a 0.5% (w/w) concentration in all tried formulas and stirred continuously until complete dissolution. The lipid phase was then dispersed in deionized water preheated at 60°C in drop wise manner with continuous stirring. The dispersion was maintained under stirring at room temperature for 2 hours to solidify the lipid droplets. The dispersion was then homogenized at 13,000 rpm for 1 min. using homogenizer (GLH850, Omni Inc, USA.) and the nano-formulation was finally stored at 4°C in glass vials. A Flowchart of the formulation steps and choice of the best prepared formula is illustrated in Figure 1.

Characterization of the Formulated Simvastatin Cubosome (SIM-CB)

Particle Size and Zeta Potential Measurements

Mean diameter, Zeta potential and polydispersity index (PDI) (size range of particles) of the cubosomal dispersion were determined using Malvern Zetasizer (Malvern

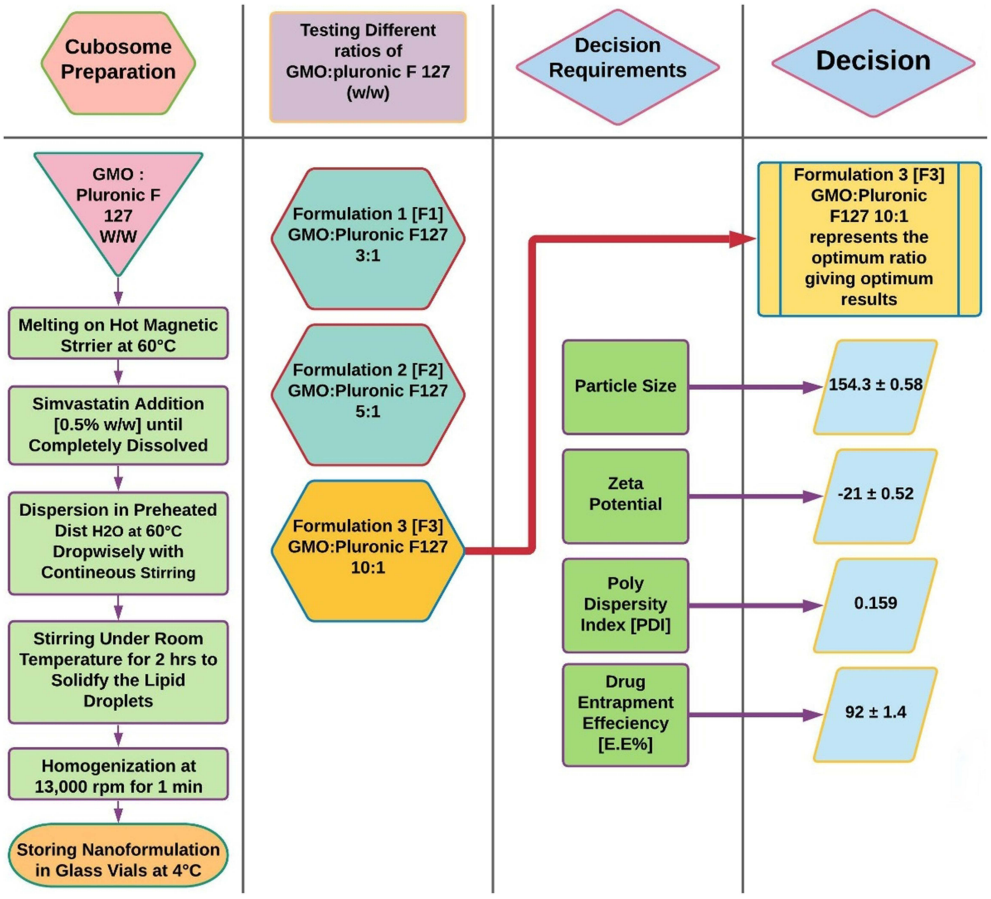

Figure 1 Flowchart of nano cubosome formulation steps and choice of the best prepared formula.

Instruments Ltd., UK). Samples were diluted (10-fold) with deionized water and measured at 25±0.5°C. The results were reported as the mean of three determinations.

Transmission Electron Microscope Examination

Morphological examination of the formulated (SIM-CB) was performed using transmission electron microscope (TEM) (JEM-1230, JOEL, USA). A droplet of cubosomes dispersion was placed on a carbon-coated copper grid, and the excess fluid was removed by an absorbent filter paper. The samples were stained with 1% sodium phospho tungstate solution. After removing the excess stain, the stained sample was dried and studied using TEM.

Fourier-Transform IR Spectroscopy (FT-IR)

Physical loading of SIM into cubosome was confirmed using (FTIR) spectroscopy (Shimadzu, Japan). Samples were prepared in potassium bromide (KBr) discs. IR spectra for free simvastatin (SIM) and Simvastatin-loaded cubosome (SIM-CB) were obtained in the spectral region 450–4000 cm^{-1}.

Determination of the Drug Content

1 mL of (SIM-CB) dispersion was diluted with 9 mL methanol. The solution was sonicated for 2 min. and filtered through 0.45 µm syringe filter, followed by dilution and analysis at wavelength of 238 nm using UV-visible spectrophotometer (Shimadzu UV-1700, Japan). The experiments were performed in triplicates and the mean was considered.

Drug content = (amount of drug obtained/amount of drug added) ×100.[32]

Entrapment Efficiency (EE %)

Estimation of Free Drug

The free amount of SIM was estimated by placing 1mL dispersion in a dialysis bag (cellulose membrane: average flat width 9 mm (0.35 inch; Sigma, USA)) which was tied and placed in 100 mL of phosphate buffer (pH 7.4): ethanol (60:40) and kept at 37°C in a shaking water bath (50 rpm). Samples were analyzed by measuring the absorbance at 238 nm using a UV-visible spectrophotometer (Shimadzu UV-1700) after suitable dilution. The experiment was performed in triplicates and the mean was reported.

Estimation of Encapsulated Drug

Meanwhile, the encapsulated SIM amount was estimated by obtaining the formulation residue in the dialysis membrane after estimation of the free SIM content. The quantity left behind in the dialysis membrane was added with methanol to dissolve the nano dispersion and filtered using a 0.45 µm syringe filter. The samples were analyzed at 238 nm after suitable dilution. The experiment was performed in triplicates, and the mean percentage was reported. The percentage of drug entrapment was calculated as follows:

% Drug entrapment = (Amount of encapsulated drug present/Total amount of drug present) × 100.[33]

In vitro Drug Release

One milliliter of freshly made cubic nanoparticle suspension (equivalent to 0.92 mg SIM) was added to a dialysis bag, suspended in a flask containing 100 mL phosphate buffer (pH 7.4):ethanol (60:40), and kept at 37 ±0.5°C in a shaking water bath at 50 rpm. A total of 5 mL medium was withdrawn at specific time periods (0.5, 1, 2, 3, 4, 5, 6, 8, 10, and 12 h). The withdrawn samples were filtered through a 0.22 µm membrane filter (Whatman Inc., USA), and 5 mL filtrate was prepared in up to 100 mL phosphate buffer. The samples were analyzed by measuring the absorbance at 238 nm to calculate the percentage of cumulative SIM release. The experiment was performed in triplicates, and the mean was calculated.

Cytotoxicity Assay

Cell viability was assessed using sulphorhodamine assay (SRB), as previously established.[34] Briefly, MCF-7 cell suspension ($5x10^3$) was aliquoted in a 96-well plate and incubated in complete medium for 24 h to ensure the attachment of cells. The cells were then incubated with 100 µL logarithmic dilutions of SIM and SIM-CB containing SIM concentrations of 0.01–100 µmol for 48 h at 37°C. The same procedure was performed using 100 µL logarithmic dilutions of equivalent volumes of vacant cubosome dispersion to check its cytotoxic effect. All treated cells were then fixed by replacing the media with 150 µL 10% TCA and incubation at 4°C for 1 h. The TCA solution was removed, and the cells were washed 5 times with distilled water. Aliquots of 70 µL SRB solution (0.4% w/v) were added, and the cells were incubated in darkness at room temperature for 10 min. The plates were washed with 1% acetic acid and allowed to air-dry overnight. Then, 150 µL TRIS (10 mM) was added to dissolve the protein-bound SRB stain. Absorbance was measured at 540 nm using BMG LABTECH®-FLUOstar Omega microplate reader (Ortenberg, Germany). The mean value

of three samples for each compound at each concentration was determined as the percentage of cell viability: (optical density (OD) of treated cells/OD of control cells) ×100. The half-maximal inhibitory concentration (IC_{50}) and confidence interval (CI) of each compound were then calculated using dose-response (inhibitory) curve-fitting models (GraphPad Prism software, version 9.1).

Apoptosis Detection by Flowcytometry

MCF7 cells were plated ($1x10^6$ cells/well) in six-well plates and allowed to attach overnight. Cells were then incubated with SIM, SIM-CB at IC_{50} doses or either compound plus Vitamin E (100μM), for 48 hours for analysis of apoptosis stages. Annexin V-FITC apoptosis detection kit (Abcam, CA, USA) was used according to the manufacturer's protocol. Briefly after treatment, adherent and floating cells were collected, washed with phosphate-buffer saline (PBS) and resuspended in 100 μL binding buffer. Then, 5 μL FITC Annexin V and 10 μL PI (propidium iodide) were added to cell suspensions, and incubated in darkness (20 min., room temperature). 400 μL binding buffer was added to cells which were analyzed by flow cytometry. Novocyte benchtop flow cytometer (ACEA, USA) and Novocyte express software were used to analyze the data. Apoptotic and necrotic cells were analyzed, and apoptotic stages were determined. Labeling patterns identified different cell populations; where FITC negative and PI negative cells denoted viable cells; FITC positive and PI negative denoted early apoptotic cells; FITC positive and PI positive denoted late apoptotic cells and FITC negative, PI positive represented necrotic cells.

Cell Cycle Analysis

Cell cycle arrest was also analyzed by flow cytometry. Briefly, MCF-7 cells were seeded in six-well plates overnight. Then, the cells were treated with SIM or SIM-CB at IC_{50} doses or with either compound plus vitamin E for 48 h. The cells were then trypsinized, washed with PBS, and fixed by storage in ice-cold 70% ethanol overnight at −20°C. After fixation, the cells were washed and incubated in 500 μL PBS, DNase free RNAse A (20 μg/mL final concentration), and PI (50 μg/mL final concentration) for 40 min in darkness at room temperature. Finally, the cells were analyzed using a NovoCyte flow cytometer (Acea Biosciences, USA). Cell cycle phases were investigated by measuring the cell uptake of PI.

Determination of Apoptotic Activity: Caspase 3 and Bcl-2 Activity

MCF-7 cells ($5x10^5$) were cultured in 6-well plates and treated with IC_{50} doses of SIM, SIM-CB or either compound with vitamin E for 48 hours. Cells were then trypsinized and centrifuged (3000 rpm, 15 min.). The cell pellet was lysed using cell lysis buffer (Invitrogen, USA) with protease inhibitor at 4°C for 1hr, followed by centrifugation (3000 rpm for 20 min). Lysates were used to determine the levels of apoptotic markers by ELISA technique: Caspase-3 (Sinogeneclon, Catalog number:SG-10396, China. Intra-assay CV < 8% and Inter-assay precision CV < 10%) and Bcl-2 (Sinogeneclon, Catalog number:SG-1040, China, Intra-assay CV < 8% and Inter-assay precision CV < 10%) following manufacturer's protocol. Absorbance was measured at 450 nm using a microplate reader (BioTek Synergy, USA).

Detection of Ferroptosis Potential: Determination of GPX4 Enzyme Level

To test the ferroptosis activity of the formulated SIM-CB, Human glutathione peroxidase 4 (GPX4) enzyme was detected by ELISA technique using the kit (Bt-Laboratory, China, catalog number: E6887Hu, Intra-assay CV < 8% and Inter-assay precision CV < 10%) following manufacturer's protocol. Briefly, MCF-7 cells ($5x10^5$) were cultured in 6-well plates and incubated with the compounds: SIM, SIM-CB at IC_{50} doses or with either compound plus vitamin E for 48 hours. Cells were then collected and centrifuged at 3000 rpm for 15 min. The cell pellet was lysed as previously mentioned and cell lysate was used to detect GPX4 level by measuring the optical density at 450 nm within 10 minutes after adding the stop solution using a microplate reader (BioTek synergy, USA).

Detection of Intracellular Reactive Oxygen Species (ROS) Level

Levels of intracellular ROS were measured using the dichloro dihydro fluorescein diacetate (DCFH-DA) detection kit (Sigma, St. Louis, MO, USA, catalog number: MAK145) according to the manufacturer's protocol. MCF-7 cells were seeded in 96-well plates at a density of $5×10^3$ and treated with SIM, SIM-CB or either of the two compounds plus vitamin E for 48 hours. After treatment, medium was removed and cells were incubated with 10 μM of DCFH-DA and 100 μL Hank's buffered salt solution (HBSS, Lonza, E.U.) for 30 min at 37°C. ROS levels were measured using a microplate reader (BioTek Synergy, Ex: 490 nm, Em: 570 nm).

Quantification of Malondialdehyde (MDA) and Reduced Glutathione (GSH) Levels

MCF-7 cells ($5x10^5$) were cultured in 6-well plates and incubated with the treatments: SIM, SIM-CB, or either compound plus vitamin E for 48 hours using IC_{50} doses. The cells were collected and lipid peroxidation was quantified by detecting Malondialdehyde (MDA) levels in MCF-7 control (untreated) and treated cell lysates according to the established colorimetric method.[35] Intracellular GSH level was determined according to Ellman's method.[36] Briefly, MCF-7 cells ($5x10^5$) were cultured in 6-well plates and incubated with the treatments for 48 hours. The absorbance was measured at 412 nm using Shimadzu RF 6000 spectrophotometer. The protein content of MCF-7 cells was determined using Pierce BCA protein assay kit (Thermo scientific, USA, catalog number: 23227) following manufacturer's protocol.

Statistical Analysis

Data analysis was performed using one-way analysis of variance (ANOVA) or two-way ANOVA followed by post-hoc Tukey's test to compare the means of multiple groups. A *p*-value less than 0.05 was considered statistically significant. All experiments were performed in triplicates and results were presented as; mean ± standard deviation (SD) for continuous variables and mean with confidence interval CI for the IC_{50} doses. Statistical analysis was performed using GraphPad Software (San Diego, California USA version 9.1.0.)

Results

Formulation and Characterization

Particle size detection showed that SIM-loaded cubosomes (SIM-CB) were successfully formulated in the nano size range. Formulations ranged from 109.3 ± 0.51nm to reach a size of around 154.3 ± 0.58 nm in formula F3, which suited the targeted size. All prepared formulas exhibited a negative zeta potential from −5.08 ± 0.27 mv in F1 and reaching to −21 ± 0.52 mv in formula F3, which denotes the highest stability. PDI examination of the three formulas revealed a particle size distribution of less than 0.2, which indicates the homogenous mono dispersion of the prepared formulations. Based on these results, Formula F3 of SIM-CB (1:10 w/w GMO: Pluronic F127) achieved the targeted size, homogeneity, and the highest stability of the dispersion. This result also agrees with previous studies that have found that cubosomes of this composition ratio have acceptable physicochemical properties and efficiently enhance the solubility and activity of poorly absorbed drugs.[37] Moreover, F3 of SIM-CB exhibited the highest EE (92% ± 1.4%). Consequently, formula F3 SIM-CB was the formula used in all the following experiments. Table 1 presents the detailed data of the used compositions and the resulting physical properties of all the formulas.

Morphology of SIM-CB

TEM analysis confirmed the cubosome was in the nano size with a smooth surface and uniform size distribution. Magnification of a single particle showed an internal cage-like cubosome structure where drug molecules are dispersed uniformly throughout the polymer matrix as shown for the selected formula F3 in Figure 2.

FT-IR Analysis

FT-IR spectra of pure simvastatin showed characteristic peaks at 3545 cm^{-1} and 3749 cm^{-1} denoting (O−H stretch vibration), 2960 cm^{-1} (C−H stretch vibration) and 1730 cm^{-1}, 1164 cm^{-1} and 1066 cm^{-1}denoting (stretch vibration of −C−O and −C=O functional groups). FT-IR analysis of SIM-CB showed the characteristic spectrum peaks of Pluronic F-127 at 1200–1000 cm-^{1} range denoting stretching vibration at the C-O-C region. Most importantly, it showed the preserved peaks of SIM, but with a slight shift and decreased peak intensity of the OH group of simvastatin, while the peak of C=O group disappeared, denoting

Table 1 Composition and Observed Characteristics of Simvastatin-Loaded Cubosomes

Formula	Components			Characterization			
	GMO: Pluronic F 127 Ratio	SIM%	Water %	Particle Size	PDI	Zeta Potential	E.E.%
F1	3:1	0.5%	To 100%	109.3±0.51	0.12	−5.58±0.31	64.3±0.65
F2	5:1			143.6±1.55	0.119	−5.08±0.27	72.4±0.9
F3	10:1			154.3±0.58	0.159	−21±0.52	92±1.4

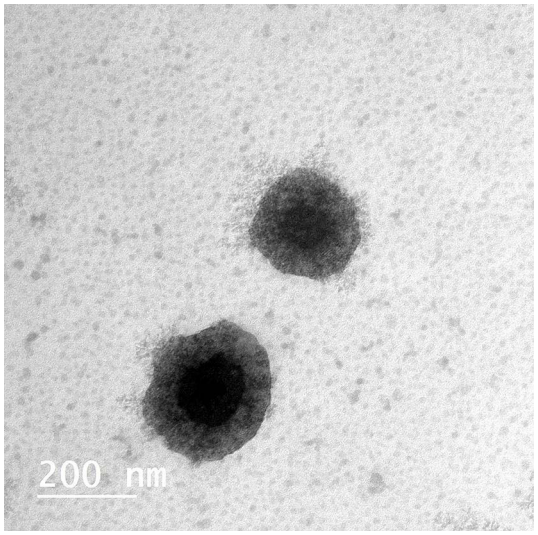

Figure 2 Transmission electron microscope photo micrographs of SIM-CB.

successful interaction between O-H of GMO and the C=O of Simvastatin. This confirms that GMO shows a remarkable tendency to interact with Simvastatin (Figure 3A).

Entrapment Efficiency& in vitro Drug Release

The formulated cubosomes showed variation in simvastatin entrapment, with entrapment efficiency starting from 64.3 ± 0.65 in F1 and peaked in Formula (F3) which exhibited the highest EE (92% ± 1.4%), due to the high concentration of the lipid component. Meanwhile, the in vitro release profiles for the raw crystalline SIM and formula F3 with SIM-CB were notably different (Figure 3B). Raw SIM was rapidly released in the first hours to be almost completed after 8 hours. Whereas, SIM-CB revealed a remarkable gradual and controlled release of simvastatin, compared to free SIM. Where nearly 42% of SIM release was achieved after 6 hours then the drug release was gradually increased to reach 92% by 12 hrs (Figure 3B). This release pattern is expected due to the high affinity of SIM with the hydrophobic domain in cubosomes, consuming more time to escape from the nanoparticles and thus allowing a sustainable effect without rapid total release. Moreover, this cumulative release is satisfactory, considering the known poor solubility of SIM.

Cytotoxicity

SRB assay confirmed the cytotoxic activity of both free SIM and SIM-CB. Where the IC_{50} of SIM was 4.8 µM, 95% CI [4.1, 5.2] SD = 0.45. Interestingly, the cubosome formulation F3, SIM-CB exhibited a significant improvement in cytotoxic activity ($p<0.05$), where compared to free SIM, the IC_{50} of SIM-CB was reduced by more than 50% to reach 2.3 µM,

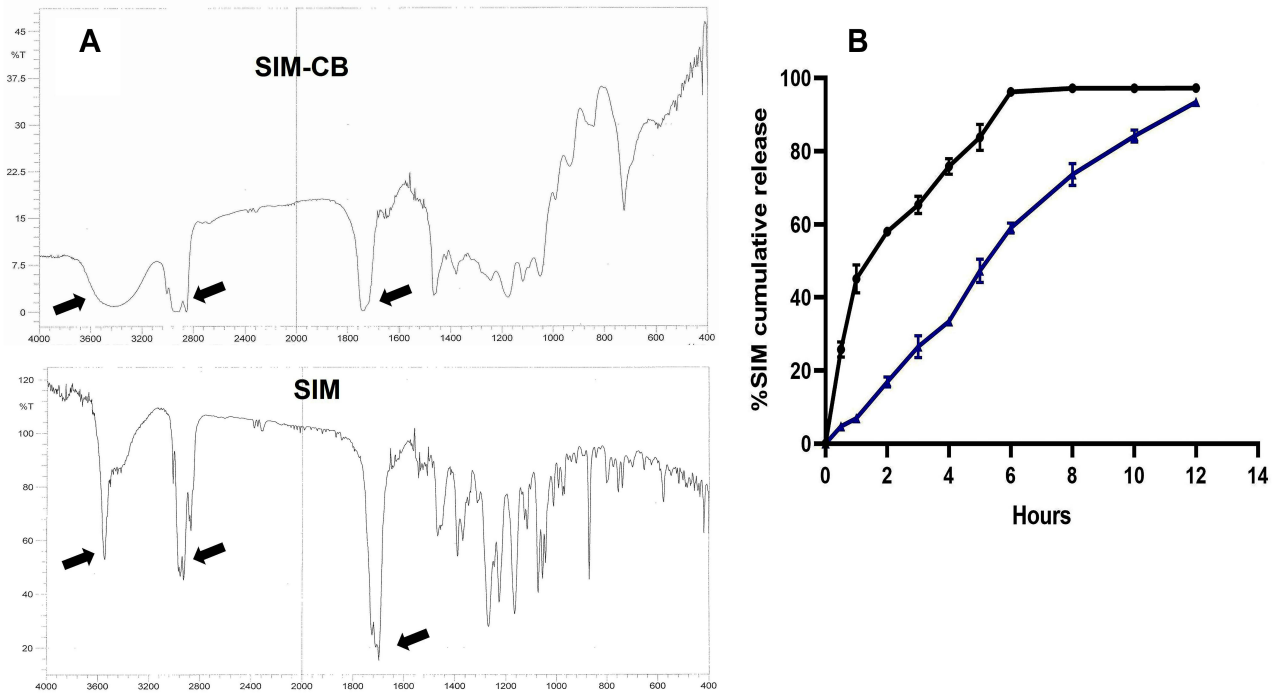

Figure 3 Analysis of SIM-CB (**A**) FTIR of free SIM and SIM-CB with arrows denoting preserved chemical entities and slight shift due to successful dispersion in cubosome system. (**B**) In vitro drug release profile of SIM and SIM-CB, showing rapid uncontrolled release of free SIM and gradual sustained release of simvastatin from SIM-CB. Blue line denotes SIM-CB and Black line denotes SIM.

95% CI [1.8, 2.7], SD = 0.34. As expected, the vacant cubosome showed approximately no cytotoxicity as more than 60% of cell viability was still maintained at 1000 µM concentration. Illustration of the cytotoxic activity of free SIM and SIM-CB is shown in Figure 4A. Meanwhile, microscopic examination of the untreated cells and cells incubated with vacant cubosomes confirmed the cell viability (Figure 4B and C). Whereas cells treated with SIM-CB manifested gradual change in morphology with cell shrinkage (Figure 4D) and progressive increase in apoptotic cells by the end of treatment (Figure 4E).

Apoptosis Analysis

Flow cytometric analysis of apoptosis stages revealed that after 48 hours, SIM and SIM-CB significantly increased total deaths of MCF-7 cells by nearly 4- and 9-fold increase respectively, compared with the untreated control cells. Two-way ANOVA analysis showed that SIM-CB significantly increased total deaths by nearly the double (13.7 ± 0.4%), compared to free SIM (6.4 ± 0.21%) ($p < 0.001$), with increase in total apoptosis ($p < 0.05$) and significant elevation of late apoptosis stage by nearly 5 folds($p < 0.0001$). Vitamin E had a moderate significant inhibitory effect on total deaths of SIM-CB, however, even when vitamin E was added, SIM-CB remained significantly more cytotoxic than free SIM alone ($p < 0.001$). Moreover, there was no significant difference between SIM-CB alone and SIM-CB with vitamin E, regarding total apoptosis and late apoptosis stages, which supports that vitamin E can affect total death by a mechanism other than apoptosis alone. Detailed Illustrations of apoptosis and the corresponding statistical analysis are shown in Figure 5.

Cell Cycle Analysis

Control untreated cells showed quick proliferative stages with percentage values of 47.3% ± 1.38, 27% ± 1.1 and 19.48% ± 0.9 for G_1, S and G_2 phases, respectively. Two-way ANOVA analysis showed that SIM treatment decreased S phase (24.3% ± 0.9) and G_2 phase (12.8% ± 2.2) but the decrease was not significant from that of control cells. Interestingly, treatment with the formulated SIM-CB caused significant changes in cell cycle phases, where it caused significant accumulation in G_1 phase (68.6% ± 1.4) that was significantly higher than that of control and free SIM ($p < 0.05$). Also, it caused significant reduction in S phase (13.2% ± 1.02) when compared to control and free SIM ($p < 0.001$) and significant reduction in G_2 phase (9.6% ± 0.68) as compared to control. Vitamin E did not significantly alter the activities of SIM-CB except in the G_2 phase which was decreased. Detailed Illustrations of cell cycle stages and the corresponding statistical analysis are shown in Figure 6.

Effect on Caspase 3 and Bcl-2 Enzymes

SIM and SIM-CB significantly increased the apoptotic enzyme Caspase 3 level as compared to control. One-Way

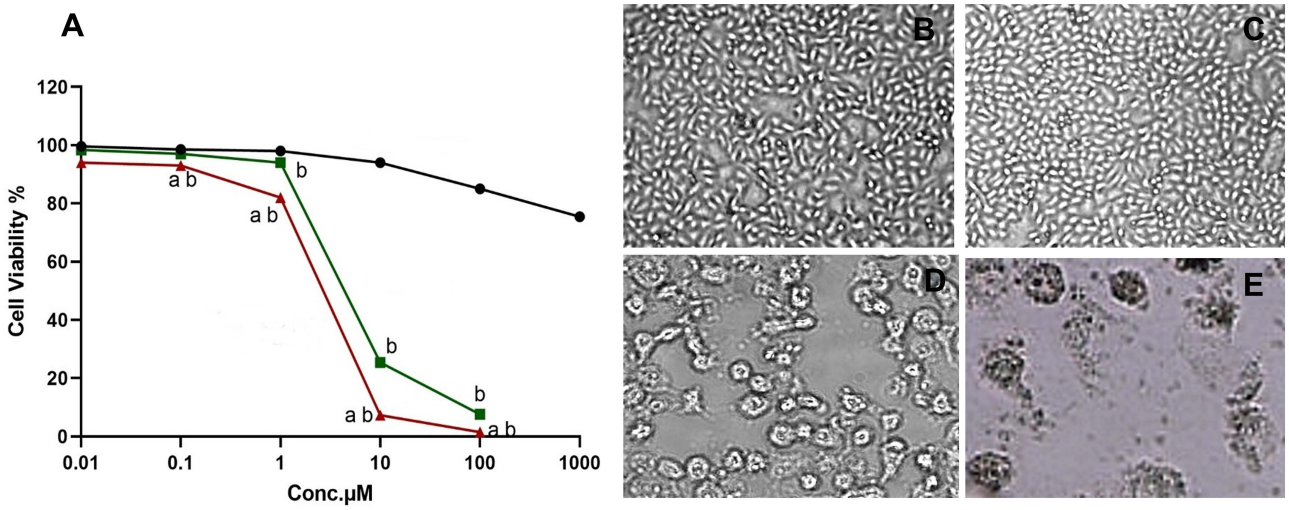

Figure 4 Cytotoxicity Assessment (**A**) Cytotoxicity analysis of Free SIM (SIM), vacant Cubosome (CB) and SIM- loaded cubosome (SIM-CB) on MCF-7 cell line after 48 hours: values are means of three independent experiments for each concentration. $p < 0.05$ was considered statistically significant. [a]p Denotes statistical significance versus SIM. [b]p Denotes statistical significance versus vacant cubosome. (**B** and **C**) Photomicrographs showing normal spindle shaped MCF-7 cells of Control untreated cells and after treatment with vacant cubosome (NC) denoting absence of cytotoxicity of vacant cubosome (Magnification X40). (**D** and **E**) Photomicrographs showing MCF-7 cells after treatment with SIM-CB. (**D**) Cells manifested progressive altered morphology to become smaller in size, with cell and cell membrane shrinkage and (**E**) increased damaged apoptotic cells after 48 hours of treatment with SIM-CB. (Magnification ×100).

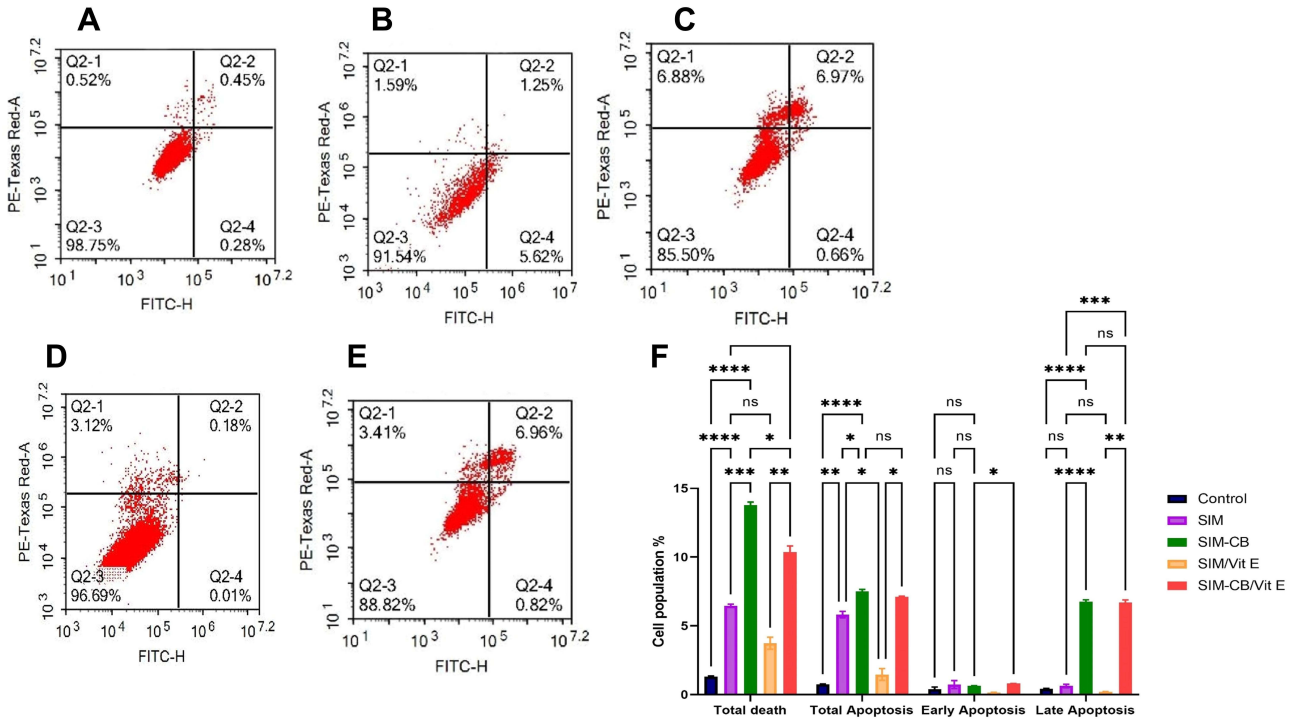

Figure 5 Apoptosis analysis using Annexin V/Propidium iodide apoptosis assay: (**A**) Control untreated cells (**B**) Free SIM treated cells (**C**) SIM-CB treated cells (**D**) SIM and Vitamin E treated cells (**E**) SIM-CB and Vitamin E treated cells. (Q2-3 denotes viable cells; Q2-4 denotes cells at early apoptotic stage; Q2-2 denotes late apoptotic stage and Q2-1 denotes necrotic cells. (**F**) Comparative statistical analysis of apoptosis and total cell deaths using Two- way ANOVA followed by post-hoc Tukey's test. Data are represented as mean ± SD (* significant difference at $p < 0.05$, **Significance at $p < 0.01$, ***Significance at $p < 0.001$, ****Significance at $p < 0.0001$). Tests were repeated in Triplicates.

Abbreviation: ns, not significant.

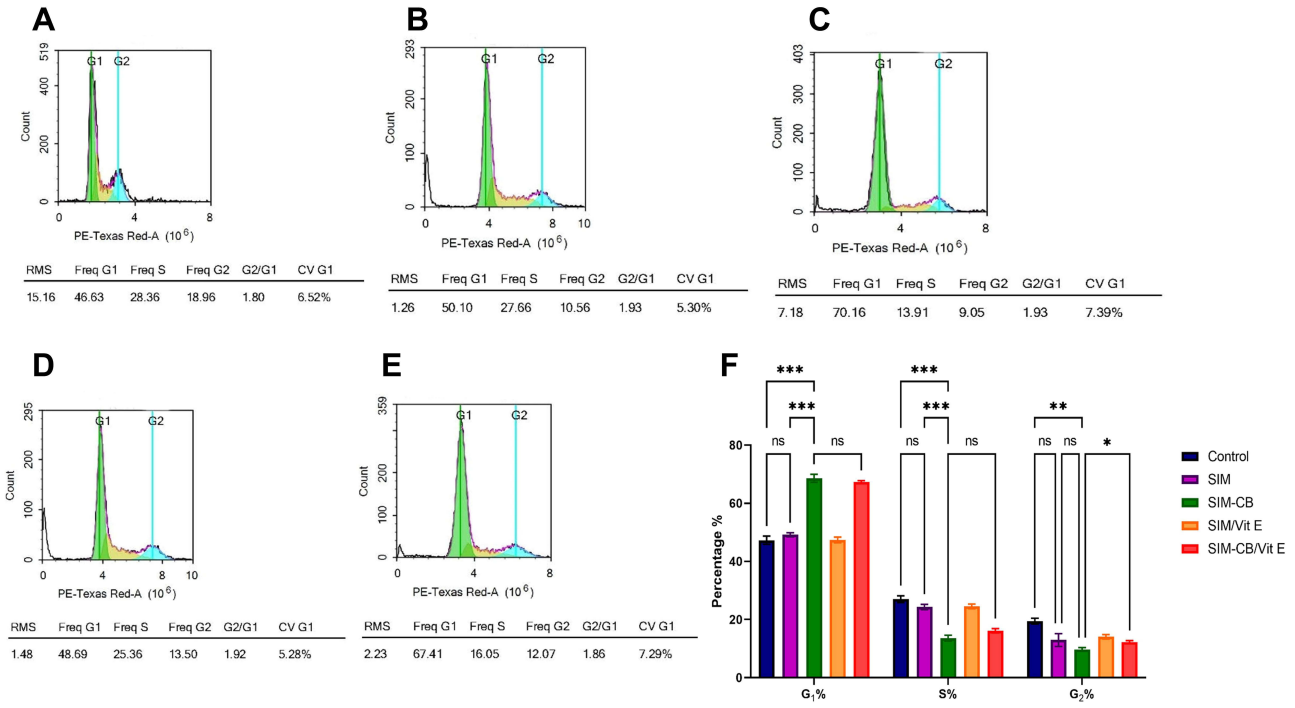

Figure 6 Cell cycle analysis using Propidium iodide assay: (**A**) Control untreated cells (**B**) Free SIM treated cells (**C**) SIM-CB treated cells (**D**) SIM and Vitamin E treated cells (**E**) SIM-CB and Vitamin E treated cells. (**F**) Comparative statistical analysis of cell cycle phases using Two- way ANOVA followed by post-hoc Tukey's test. Data are represented as mean ± SD (* denotes significance at $p < 0.05$, **Significance at $p < 0.01$, ***Denotes significance at $p < 0.001$). Tests were repeated in Triplicates.

Abbreviation: ns, not significant.

ANOVA test showed remarkable changes upon treatment with SIM and SIM-CB. SIM-CB significantly increased caspase 3 level (7.5 ± 0.33 ng/mL) compared to free SIM (4.2 ± 0.21 ng/mL) ($p < 0.0001$). The addition of vitamin E to either drug did not significantly decrease their effect, however the stimulatory effect of SIM-CB on caspase enzyme remained more significantly active compared to SIM plus vitamin E at $p < 0.0001$ (Figure 7A). Meanwhile, both SIM and SIM-CB significantly decreased the antiapoptotic Bcl-2 protein. However, treatment with SIM-CB had significantly more powerful inhibitory effect on Bcl-2 (2.35 ± 0.12 ng/mL) compared to free SIM (3.51 ± 0.23 ng/mL) at $p < 0.0001$. This effect was not altered by vitamin E (Figure 7B).

Effect on Glutathione Peroxidase 4 Enzyme (GPX4)

ANOVA test revealed remarkable effects of treatments, where SIM-CB significantly decreased GPX4 level (3.3 ± 0.13 ng/mL) compared to treatment with free SIM (4.2 ± 0.14 ng/mL) at $p < 0.01$. Vitamin E decreased the inhibitory effect of simvastatin on GPX4 level in free SIM (4.9 ± 0.25 ng/mL) and SIM-CB (3.6 ± 0.14 ng/mL), respectively. However, SIM-CB formula was more resistant to vitamin E effect, where treatment with SIM-CB caused significantly more inhibitory effect on GPX4, compared to either SIM alone or SIM with vitamin E at ($p < 0.001$) (Figure 7C).

Effect on Reactive Oxygen Species (ROS)

SIM-CB significantly caused a twofold increase in ROS level compared to untreated cells and a significant 50% increase compared to treatment with free SIM ($p < 0.0001$). Vitamin E caused significant 30% decrease of ROS levels compared to treatment with Free SIM or SIM-CB alone. However, despite the addition of vitamin E, SIM-CB formula remained significantly more powerful to generate ROS compared to free SIM ($p < 0.0001$). Figure 8A.

Effect on Intracellular MDA and GSH Levels

SIM-CB formula caused a significant fourfold increase in MDA levels compared with untreated cells and around 1.5-fold increase compared to free SIM ($p < 0.0001$). Adding vitamin E significantly decreased MDA by around 50% and 30% when added with SIM and SIM-CB formula, respectively. However, SIM-CB remained significantly more powerful to induce lipid peroxidation compared to SIM ($p < 0.0001$) (Figure 8B). In coordination, SIM-CB significantly decreased intracellular GSH level (2.1 ± 0.1 µmole/mg) as compared to free SIM (2.6 ± 0.14 µmole/mg) ($p < 0.05$). Meanwhile, vitamin E slightly increased the GSH levels. However, its effect on GSH level was not significantly different from each treatment alone (Figure 8C).

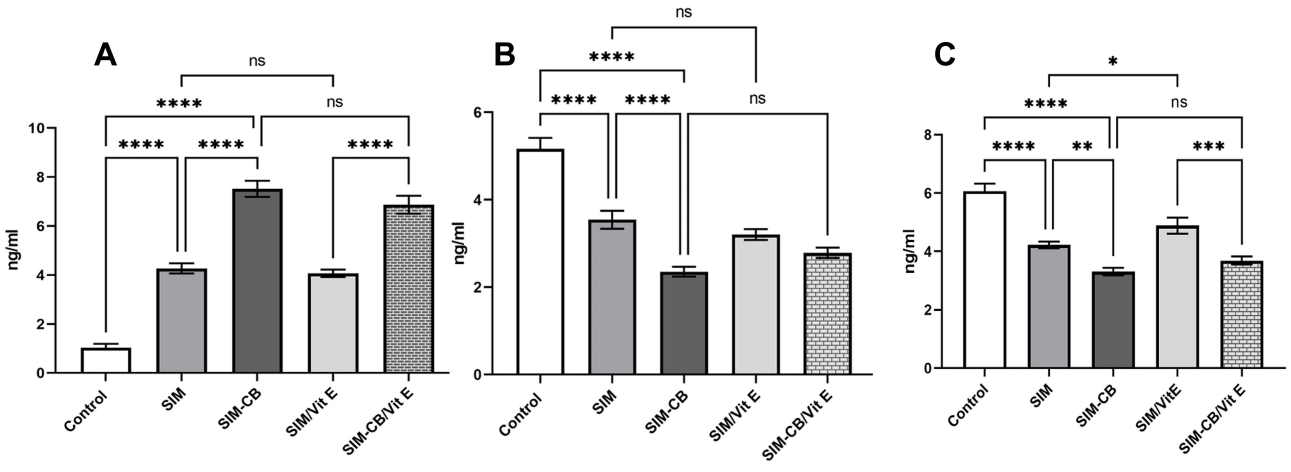

Figure 7 Effect of different treatments on (**A**) Caspase3 levels (**B**) Bcl-2 levels (**C**) GPX4 level in MCF-7 cell line: Statistical analysis was performed using One-way ANOVA followed by post-hoc Tukey's test. Data are represented as mean ± SD (*p Denotes significance at $p < 0.05$, **Denotes significance at $p< 0.01$, ***Denotes significance at $p< 0.001$, ****Denotes significance at $p < 0.0001$. Tests were repeated in triplicates).
Abbreviation: ns, not significant.

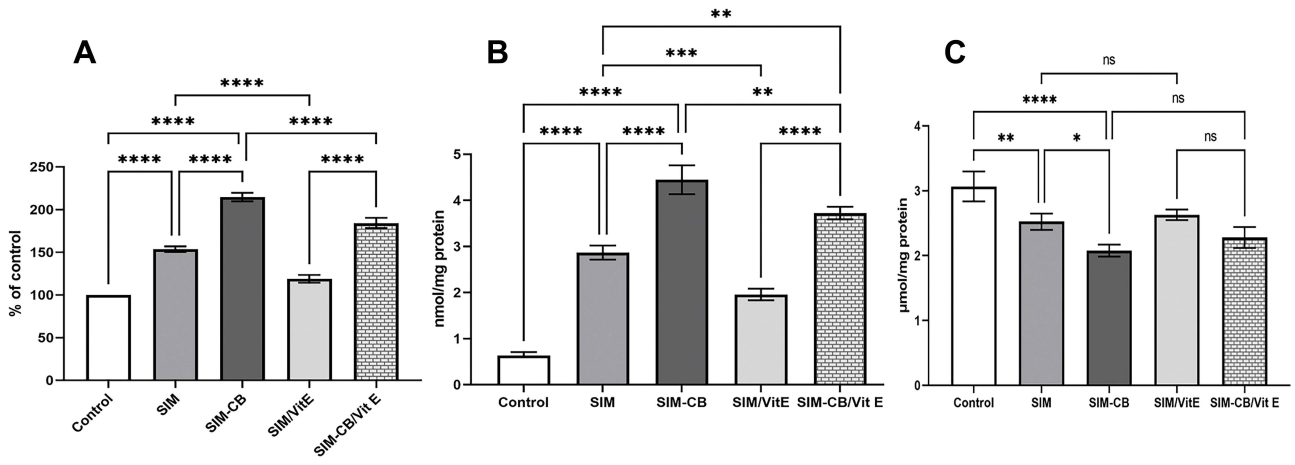

Figure 8 Effect of different treatments on (**A**) ROS levels (**B**) MDA levels (**C**) GSH level in MCF-7 cell line: Statistical analysis was performed using One-way ANOVA followed by post-hoc Tukey's test. Data are represented as mean ± SD (* p denotes significance at $p < 0.05$, **Denotes significance at $p < 0.01$, ***Denotes significance at $p < 0.001$, ****Denotes significance at $p < 0.0001$. Tests were repeated in triplicates).
Abbreviation: ns, not significant.

Discussion

Chemotherapy is often hindered by multidrug resistance. Therefore, a continuous search for new agents that withstand this challenge is highly needed. The off-label anticancer activity of statins is increasingly reported in different cancer types.[38] However, the wide mechanistic investigation and application of SIM as an anticancer agent are still limited by its poor aqueous solubility, rapid metabolism, and excretion, which drastically affect the delivery and persistence of adequate concentrations in tumor sites.[19] The incorporation of nanotechnology introduces remarkable solutions for the improvement of solubility, absorption, and stability of different agents.[31,39] Moreover, this process enhances the therapeutic activity of promising compounds through improving their solubility and adequate delivery.[22,40]

Therefore, in this study, we formulated SIM in a SIM-CB formula. We tested the cytotoxic activity of free SIM and SIM-CB on MCF-7 cells and investigated ferroptosis as a possible additional mechanism contributing to SIM anticancer actions. In the present study, cubosome formulation was intentionally selected because cubosomes are biocompatible and highly stable. They have a uniquely large hydrophobic volume which enables efficient loading of lipophilic drugs such as SIM.[21] In addition, in cancerous cells, the large surface area of cubosomes allows for larger drug payload and controllable release, improving drug concentrations and avoiding premature leakage.[29] The carrier size, shape, and zeta potential are crucial criteria to accomplishing the successful delivery of drugs to the targeted tumor type without compromising the stability, non-specific entrapment in other cells, or the phagocytic system.[41] Accordingly, we modulated the GMO: Pluronic F127 ratios, and an evident relation was observed between the increase in GMO amount and improvement in particle size, PDI, and zeta potential to meet our needed model. The suitable formula was accomplished in formula F3. Transmission electron microscopy analysis confirmed the successful formulation of cubosomes of around 154 nm. This size accomplishes multiple advantages because particles less than 200 nm are ideal to avoid capture and clearance by the mononuclear phagocytic system.[42] Likewise, this size selectively fits in the leaky large pores of breast tumor (200 nm) while preventing passage through normal blood vessels,[43] thus reducing the formula toxicity. Additionally, this size accomplished a diminished electrostatic repulsion due to the small ratio of cubosome to the pore size of vessel wall.[44] The PDI was less than 0.2, which is a favorable value for uniform distribution and homogeneity[45] and highly acceptable for lipid-based carriers.[46] Simultaneously, a zeta potential higher than −20 mv guarantees stability and the ease of dispersion.[47] The best zeta potential was achieved in SIM-CB F3, denoting a high stability while ensuring prevented aggregation. Meanwhile, Fourier-transform infrared analysis showed preserved peaks of SIM in SIM-CB, in agreement with previous literature.[48]

Moreover, formula F3 of SIM-CB showed the highest EE, with the GMO concentration providing a suitable environment to entrap SIM in adequate levels. These results agree

with those of previous studies.[8,49] Correspondingly, the SIM-CB formula showed a gradual and controlled release of SIM, which was almost depleted after 12 h, denoting the high dispersion of SIM in the lipid matrix. This finding agrees with that of previous studies[49] and is acceptable given the extreme poor solubility of SIM. Moreover, this event proves the sustained-release capability of the formulated SIM-CB.

Upon testing the cytotoxic activity of SIM-CB, cytotoxicity test confirmed the significant improvement of the therapeutic potential of SIM-CB, and its IC_{50} was less than half that of the free SIM. Meanwhile, the absence of cytotoxicity for vacant cubosomes supports the biocompatibility of the novel formula. Notably, this result accounts for multiple advantages of SIM-CB because it denotes the magnification of SIM cytotoxic activity at low drug concentrations while minimizing the chance of unwanted adverse effects.

In the analysis of the cytotoxic mechanisms of SIM-CB, the present study showed that SIM-CB drastically increased the total, apoptotic, and necrotic deaths. Compared with the free SIM, SIM-CB caused the significant accumulation of cells in the G1 phase, preventing cellular transition to the S and G2 checkpoint phases, which caused remarkable increases in the late and total apoptosis.[50] The enhanced cytotoxic activity of SIM-CB can be attributed to the remarkable improvement of SIM solubility and its controlled release from the cubosomes. These results agree with those of the recent study of Shen et al,[51] which illustrated the effect of SIM on cell cycle and apoptosis.

The inhibitory effect of vitamin E against anticancer agents was recently spotted.[52,53] Vitamin E decreases cellular ROS generation to interact with oxidative stress responses and the consequent signaling pathways in tumor cells.[50,51] In this study, vitamin E partially halted the death activity of free SIM and SIM-CB. However, the SIM-CB formula significantly resisted the effect of vitamin E compared with free SIM. SIM-CB showed significantly higher total deaths, late apoptotic signals, and cell arrest than SIM alone or SIM plus vitamin E. This efficacious effect of SIM-CB may be partially attributed to the improved interaction with the phospholipid cell membranes[54] due to the presence of lipophilic moiety in cubosomes, allowing the prolonged interaction with the cell membranes.

Cancer progression primarily depends on the balanced levels of proapoptotic proteins, such as Bcl-2-associated X protein, and antiapoptotic proteins, including Bcl-2.[55] Meanwhile, the caspase cascade complements the apoptosis process via activating the caspase-3 to execute the final steps of apoptosis. In the present study, SIM and SIM-CB remarkably activated caspase-3 and reduced the Bcl-2 levels. However, the apoptotic activity of SIM-CB was significantly high. Moreover, it elicited a significantly high resistance to the inhibitory effect of vitamin E. These results are in line with those of recent studies, which revealed the apoptotic activity of SIM via modulating caspase 3 and Bcl-2 levels.[51,56]

In addition to apoptosis, increasing reports imply that lipophilic statins are ferroptosis inducers.[57,58] Ferroptosis majorly depends on creating imbalance between lipid hydroperoxide detoxification mechanisms and lipid ROS accumulation. Pushing this balance in favor of lipid hydroperoxide accumulation, activates ferroptosis and cell death. Simultaneously, proper functionality of glutathione peroxidase 4 (GPX4) is the core of keeping ferroptosis checked. Where GPX4 uniquely reduces phospholipid hydroperoxides and cholesterol hydroperoxides to interrupt lipid peroxidation chain reaction and ferroptosis, whereas inhibiting GPX4 expression or levels activates ferroptosis.[15]

Emerging evidence suggests that statins can induce ferroptosis through reducing GPX4 levels and/or activity.[59,60] However, to the best of our knowledge, there are little data about the effect of SIM on GPX4 enzyme in breast cancer. Indeed, the present study confirmed that SIMreduces GPX4 levels in MCF-7 cells, where the inhibitory effect of SIM-CB was significantly higher than that of free SIM. Proper GPX4 function requires an adequate supply of reduced GSH to provide thiol group as an electron donor, and subsider of ROS effect.[61] Hence, GSH depletion inhibits GPX4 activity and increases intracellular lipid peroxides, resulting in increased ferroptosis. The results of the present study go in line with this theory where both SIM and SIM-CB significantly depleted GSH levels, and drastically increased ROS and MDA production. In coordination, the effect of SIM on MDA, ROS and GSH levels in tumor cells has been repeatedly reported by previous studies.[9,50] Additionally, GPX4 synthesis depends on the presence of isopentenyl pyrophosphate (IPP), a product of mevalonate pathway, which is critical for GPX4 synthesis and maturation. Hence, decreased level of IPP results in decreased GPX4 synthesis and activated ferroptosis.[58,62] It is established that statins inhibit mevalonate pathway, leading to decreased production of IPP, which supports the presented data regarding SIM effect on GPX4 enzyme.

Finally, vitamin E was applied as a potent antioxidant and ferroptosis inhibitor to confirm the activity of SIM and SIM-CB on MCF-7 cells. In the present study, vitamin

E significantly inhibited the ROS production, reducing the effect of SIM and SIM-CB on MDA and GPX4 levels. Interestingly, SIM-CB was evidently significantly more resistant to vitamin E compared with the free SIM. This persistent activity of SIM-CB against vitamin E may be attributed to the improved and prolonged release and hence, the cumulative concentration of SIM.

Conclusion

In conclusion, the present study showed the promising and potent antitumor activity of SIM-loaded cubosomes (SIM-CB) on MCF-7 cells in vitro, compared to free SIM. The study also highlights ferroptosis as a vital contributing mechanism of SIM anticancer activity, besides apoptosis and proliferative arrest. These findings open the field for future further analysis of SIM-cubosomes in vivo, to fully unleash statins potential as anticancer agents.

Disclosure

The authors report no conflicts of interest in this work.

References

1. Sung H, Ferlay J, Siegel RL, et al. Global cancer statistics 2020: GLOBOCAN estimates of incidence and mortality worldwide for 36 cancers in 185 countries. *CA Cancer J Clin*. 2021;71(3):209–249. doi:10.3322/caac.21660
2. Kimbung S, Loman N, Hedenfalk I. Clinical and molecular complexity of breast cancer metastases. *Semin Cancer Biol*. 2015;35:85–95. doi:10.1016/j.semcancer.2015.08.009
3. Alarfi H, Youssef LA, Salamoon M, Prospective A. Randomized, placebo-controlled study of a combination of simvastatin and chemotherapy in metastatic breast cancer. *J Oncol*. 2020;2020:e4174395. doi:10.1155/2020/4174395
4. Di Bello E, Zwergel C, Mai A, Valente S. The innovative potential of statins in cancer: new targets for new therapies. *Front Chem*. 2020;8. doi:10.3389/fchem.2020.00516
5. Beckwitt CH, Brufsky A, Oltvai ZN, Wells A. Statin drugs to reduce breast cancer recurrence and mortality. *Breast Cancer Res BCR*. 2018;20. doi:10.1186/s13058-018-1066-z
6. Harborg S, Heide-Jørgensen U, Ahern TP, Ewertz M, Cronin-Fenton D, Borgquist S. Statin use and breast cancer recurrence in postmenopausal women treated with adjuvant aromatase inhibitors: a Danish population-based cohort study. *Breast Cancer Res Treat*. 2020;183(1):153–160. doi:10.1007/s10549-020-05749-5
7. Buranrat B, Suwannaloet W, Naowaboot J. Simvastatin potentiates doxorubicin activity against MCF-7 breast cancer cells. *Oncol Lett*. 2017;14(5):6243–6250. doi:10.3892/ol.2017.6783
8. Awan ZA, Fahmy A, Badr-Eldin SM, et al. The Enhanced Cytotoxic and Pro-Apoptotic Effects of Optimized Simvastatin-Loaded Emulsomes on MCF-7 Breast Cancer Cells. *Pharmaceutics*. 2020;12(7):597. doi:10.3390/pharmaceutics12070597
9. Spampanato C, DE MARIA S, Sarnataro M, et al. Simvastatin inhibits cancer cell growth by inducing apoptosis correlated to activation of Bax and down-regulation of BCL-2 gene expression. *Int J Oncol*. 2011;40(4):935–941. doi:10.3892/ijo.2011.1273
10. Jang HJ, Hong EM, Park SW, et al. Statin induces apoptosis of human colon cancer cells and downregulation of insulin-like growth factor 1 receptor via proapoptotic ERK activation. *Oncol Lett*. 2016;12(1):250–256. doi:10.3892/ol.2016.4569
11. Mou Y, Wang J, Wu J, et al. Ferroptosis, a new form of cell death: opportunities and challenges in cancer. *J Hematol OncolJ Hematol Oncol*. 2019;12(1):34. doi:10.1186/s13045-019-0720-y
12. Han C, Liu Y, Dai R, Ismail N, Su W, Li B. Ferroptosis and its potential role in human diseases. *Front Pharmacol*. 2020;11. doi:10.3389/fphar.2020.00239
13. Li J, Cao F, Yin H, et al. Ferroptosis: past, present and future. *Cell Death Dis*. 2020;11(2):1–13. doi:10.1038/s41419-020-2298-2
14. Li D, Li Y. The interaction between ferroptosis and lipid metabolism in cancer. *Signal Transduct Target Ther*. 2020;5. doi:10.1038/s41392-020-00216-5
15. Stockwell BR, Angeli JPF, Bayir H, et al. Ferroptosis: a regulated cell death nexus linking metabolism, redox biology, and disease. *Cell*. 2017;171(2):273–285. doi:10.1016/j.cell.2017.09.021
16. Bathaie SZ, Ashrafi M, Azizian M, Tamanoi F. Mevalonate Pathway and Human Cancers. *Curr Mol Pharmacol*. 2017;10(2):77–85. doi:10.2174/1874467209666160112123205
17. Sethunath V, Hu H, Angelis CD, et al. Targeting the Mevalonate Pathway to Overcome Acquired Anti-HER2 Treatment Resistance in Breast Cancer. *Mol Cancer Res*. 2019;17(11):2318–2330. doi:10.1158/1541-7786.MCR-19-0756
18. Petyaev IM. Improvement of hepatic bioavailability as a new step for the future of statin. *Arch Med Sci AMS*. 2015;11(2):406–410. doi:10.5114/aoms.2015.50972
19. Schachter M. Chemical, pharmacokinetic and pharmacodynamic properties of statins: an update. *Fundam Clin Pharmacol*. 2005;19(1):117–125. doi:10.1111/j.1472-8206.2004.00299.x
20. Abdelaziz HM, Elzoghby AO, Helmy MW, Samaha MW, Fang J-Y, Freag MS. Liquid crystalline assembly for potential combinatorial chemo–herbal drug delivery to lung cancer cells. *Int J Nanomedicine*. 2019;14:499–517. doi:10.2147/IJN.S188335
21. Chen Y, Ma P, Gui S. Cubic and hexagonal liquid crystals as drug delivery systems. *BioMed Res Int*. 2014;2014:e815981. doi:10.1155/2014/815981
22. Gaballa SA, El Garhy OH, Abdelkader H. Cubosomes: composition, preparation, and drug delivery applications. *J Adv Biomed Pharm Sci*. 2020;3(1):1–9. doi:10.21608/jabps.2019.16887.1057
23. Cytryniak A, Nazaruk E, Bilewicz R, et al. Lipidic Cubic-Phase Nanoparticles (Cubosomes) Loaded with Doxorubicin and Labeled with 177Lu as a Potential Tool for Combined Chemo and Internal Radiotherapy for Cancers. *Nanomaterials*. 2020;10(11):2272. doi:10.3390/nano10112272
24. Nazaruk E, Majkowska-Pilip A, Bilewicz R. Lipidic Cubic-Phase Nanoparticles—Cubosomes for Efficient Drug Delivery to Cancer Cells. *ChemPlusChem*. 2017;82(4):570–575. doi:10.1002/cplu.201600534
25. Hu Q, Zhang Y, Lou H, et al. GPX4 and vitamin E cooperatively protect hematopoietic stem and progenitor cells from lipid peroxidation and ferroptosis. *Cell Death Dis*. 2021;12(7):1–9. doi:10.1038/s41419-021-04008-9
26. Tavakol S, Seifalian AM. Vitamin E at a high dose as an anti-ferroptosis drug and not just a supplement for COVID-19 treatment. *Biotechnol Appl Biochem*. 2021. doi:10.1002/bab.2176
27. Kajarabille N, Latunde-Dada GO. Programmed cell-death by ferroptosis: antioxidants as mitigators. *Int J Mol Sci*. 2019;20(19):4968. doi:10.3390/ijms20194968
28. Guo C, Wang J, Cao F, Lee RJ, Zhai G. Lyotropic liquid crystal systems in drug delivery. *Drug Discov Today*. 2010;15(23–24):1032–1040. doi:10.1016/j.drudis.2010.09.006

29. Flak DK, Adamski V, Nowaczyk G, et al. AT101-loaded cubosomes as an alternative for improved glioblastoma therapy. *Int J Nanomedicine*. 2020;15:7415–7431. doi:10.2147/IJN.S265061
30. Tang X, Loc WS, Dong C, et al. The use of nanoparticulates to treat breast cancer. *Nanomed*. 2017;12(19):2367–2388. doi:10.2217/nnm-2017-0202
31. Abdel-Mageed HM, AbuelEzz NZ, Radwan RA, Mohamed SA. Nanoparticles in nanomedicine: a comprehensive updated review on current status, challenges and emerging opportunities. *J Microencapsul*. 2021;38(6):414–436. doi:10.1080/02652048.2021.1942275
32. Padhye SG, Nagarsenker MS. Simvastatin Solid Lipid Nanoparticles for Oral Delivery: formulation Development and In vivo Evaluation. *Indian J Pharm Sci*. 2013;75(5):591–598.
33. Leroux J-C, Allémann E, De Jaeghere F, Doelker E, Gurny R. Biodegradable nanoparticles — from sustained release formulations to improved site specific drug delivery. *J Controlled Release*. 1996;39(2):339–350. doi:10.1016/0168-3659(95)00164-6
34. Skehan P, Storeng R, Scudiero D, et al. New colorimetric cytotoxicity assay for anticancer-drug screening. *J Natl Cancer Inst*. 1990;82(13):1107–1112. doi:10.1093/jnci/82.13.1107
35. Buege JA, Aust SD. Microsomal lipid peroxidation. *Methods Enzymol*. 1978;52:302–310. doi:10.1016/s0076-6879(78)52032-6
36. Ellman GL. Tissue sulfhydryl groups. *Arch Biochem Biophys*. 1959;82(1):70–77. doi:10.1016/0003-9861(59)90090-6
37. Ali MA, Kataoka N, Ranneh A-H, et al. Enhancing the solubility and oral bioavailability of poorly water-soluble drugs using monoolein cubosomes. *Chem Pharm Bull*. 2017;65(1):42–48. doi:10.1248/cpb.c16-00513
38. Barbalata CI, Tefas LR, Achim M, Tomuta I, Porfire AS. Statins in risk-reduction and treatment of cancer. *World J Clin Oncol*. 2020;11(8):573–588. doi:10.5306/wjco.v11.i8.573
39. Mageed H, Ezz N, Radwan R. Bio-inspired trypsin-chitosan cross-linked enzyme aggregates: a versatile approach for stabilization through carrier-free immobilization. *BioTechnologia*. 2019;100(3):301–309. doi:10.5114/bta.2019.87589
40. Abuelezz NZ, Shabana ME, Rashed L, Morcos GN. Nanocurcumin Modulates miR-223-3p and NF-κB Levels in the Pancreas of Rat Model of Polycystic Ovary Syndrome to Attenuate Autophagy Flare, Insulin Resistance and Improve β Cell Mass. *J Exp Pharmacol*. 2021;13:873–888. doi:10.2147/JEP.S323962
41. Rizvi SAA, Saleh AM. Applications of nanoparticle systems in drug delivery technology. *Saudi Pharm J SPJ*. 2018;26(1):64–70. doi:10.1016/j.jsps.2017.10.012
42. Moghimi SM, Hunter AC, Murray JC. Long-circulating and target-specific nanoparticles: theory to practice. *Pharmacol Rev*. 2001;53(2):283–318.
43. Hashizume H, Baluk P, Morikawa S, et al. Openings between Defective Endothelial Cells Explain Tumor Vessel Leakiness. *Am J Pathol*. 2000;156(4):1363–1380. doi:10.1016/S0002-9440(10)65006-7
44. Zein R, Sharrouf W, Selting K. Physical properties of nanoparticles that result in improved cancer targeting. *J Oncol*. 2020;2020:e5194780. doi:10.1155/2020/5194780
45. Elakkad YE, Younis MK, Allam RM, Mohsen AF, Khalil IA. Tenoxicam loaded hyalcubosomes for osteoarthritis. *Int J Pharm*. 2021;601:120483. doi:10.1016/j.ijpharm.2021.120483
46. Nasr M, Younes H, Abdel-Rashid RS. Formulation and evaluation of cubosomes containing colchicine for transdermal delivery. *Drug Deliv Transl Res*. 2020;10(5):1302–1313. doi:10.1007/s13346-020-00785-6
47. Jacobs C, Müller RH. Production and characterization of a budesonide nanosuspension for pulmonary administration. *Pharm Res*. 2002;19(2):189–194. doi:10.1023/A:1014276917363
48. Singh H, Philip B, Pathak K. Preparation, Characterization and Pharmacodynamic Evaluation of Fused Dispersions of Simvastatin using PEO-PPO Block Copolymer. *Iran J Pharm Res IJPR*. 2012;11(2):433–445.
49. Krishnam Raju K, Sudhakar B, Murthy KVR. Factorial Design Studies and Biopharmaceutical Evaluation of Simvastatin Loaded Solid Lipid Nanoparticles for Improving the Oral Bioavailability. *ISRN Nanotechnol*. 2014;2014:e951016. doi:10.1155/2014/951016
50. Buranrat B, Senggunprai L, Prawan A, Kukongviriyapan V. Simvastatin and atorvastatin as inhibitors of proliferation and inducers of apoptosis in human cholangiocarcinoma cells. *Life Sci*. 2016;153:41–49. doi:10.1016/j.lfs.2016.04.018
51. Shen -Y-Y, Yuan Y, Du -Y-Y, Pan -Y-Y. Molecular mechanism underlying the anticancer effect of simvastatin on MDA-MB-231 human breast cancer cells. *Mol Med Rep*. 2015;12(1):623–630. doi:10.3892/mmr.2015.3411
52. Vivarelli F, Canistro D, Cirillo S. Co-carcinogenic effects of vitamin E in prostate. *Sci Rep*. 2019;9(1). doi:10.1038/s41598-019-48213-1
53. Diao QX, Zhang JZ, Zhao T, et al. Vitamin E promotes breast cancer cell proliferation by reducing ROS production and p53 expression. *Eur Rev Med Pharmacol Sci*. 2016;20(12):2710–2717.
54. Murphy C, Deplazes E, Cranfield CG, Garcia A. The Role of Structure and Biophysical Properties in the Pleiotropic Effects of Statins. *Int J Mol Sci*. 2020;21(22):8745. doi:10.3390/ijms21228745
55. Adams JM, Cory S. The Bcl-2 apoptotic switch in cancer development and therapy. *Oncogene*. 2007;26(9):1324–1337. doi:10.1038/sj.onc.1210220
56. Shen Y, Du Y, Zhang Y, Pan Y. Synergistic effects of combined treatment with simvastatin and exemestane on MCF-7 human breast cancer cells. *Mol Med Rep*. 2015;12(1):456–462. doi:10.3892/mmr.2015.3406
57. Dixon SJ, Stockwell BR. The Hallmarks of Ferroptosis. *Annu Rev Cancer Biol*. 2019;3(1):35–54. doi:10.1146/annurev-cancerbio-030518-055844
58. Hao S, Liang B, Huang Q, et al. Metabolic networks in ferroptosis. *Oncol Lett*. 2018;15(4):5405–5411. doi:10.3892/ol.2018.8066
59. Forcina GC, Dixon SJ. GPX4 at the Crossroads of Lipid Homeostasis and Ferroptosis. *Proteomics*. 2019;19(18):e1800311. doi:10.1002/pmic.201800311
60. Jiang W, Hu J-W, He X-R, Jin W-L, He X-Y. Statins: a repurposed drug to fight cancer. *J Exp Clin Cancer Res*. 2021;40(1):241. doi:10.1186/s13046-021-02041-2
61. Ursini F, Maiorino M. Lipid peroxidation and ferroptosis: the role of GSH and GPx4. *Free Radic Biol Med*. 2020;152:175–185. doi:10.1016/j.freeradbiomed.2020.02.027
62. Wang H, Cheng Y, Mao C, et al. Emerging mechanisms and targeted therapy of ferroptosis in cancer. *Mol Ther*. 2021:254. doi:10.1016/j.ymthe.2021.03.022